Similar cation channels mediate protection
from cerebellar exitotoxicity by exercise and inheritance

Shani Ben-Ari [a], **Keren Ofek** [a], **Shahar Barbash** [a], **Hanoch Meiri** [b], **Eugenia Kovalev** [c],
David Samuel Greenberg [a], **Hermona Soreq** [a, d, *], **Shai Shoham** [c]

[a] *Department of Biological Chemistry, The Hebrew University of Jerusalem, Jerusalem, Israel*
[b] *Department of Neurobiology, The Hebrew University of Jerusalem, Israel*
[c] *Research Department, Herzog Hospital, Jerusalem, Israel*
[d] *The Edmond and Lily Safra Center for Brain Sciences, The Hebrew University of Jerusalem, Jerusalem, Israel*

Abstract

Exercise and inherited factors both affect recovery from stroke and head injury, but the underlying mechanisms and interconnections between them are yet unknown. Here, we report that similar cation channels mediate the protective effect of exercise and specific genetic background in a kainate injection model of cerebellar stroke. Microinjection to the cerebellum of the glutamatergic agonist, kainate, creates glutamatergic excito-toxicity characteristic of focal stroke, head injury or alcoholism. Inherited protection and prior exercise were both accompanied by higher cerebellar expression levels of the Kir6.1 ATP-dependent potassium channel in adjacent Bergmann glia, and voltage-gated KVbeta2 and cyclic nucleotide-gated cation HCN1 channels in basket cells. Sedentary FVB/N and exercised C57BL/6 mice both expressed higher levels of these cation channels compared to sedentary C57BL/6 mice, and were both found to be less sensitive to glutamate toxicity. Moreover, blocking ATP-dependent potassium channels with Glibenclamide enhanced kainate-induced cell death in cerebellar slices from the resilient sedentary FVB/N mice. Furthermore, exercise increased the number of acetylcholinesterase-positive fibres in the molecular layer, reduced cerebellar cytokine levels and suppressed serum acetylcholinesterase activity, suggesting anti-inflammatory protection by enhanced cholinergic signalling. Our findings demonstrate for the first time that routine exercise and specific genetic backgrounds confer protection from cerebellar glutamatergic damages by similar molecular mechanisms, including elevated expression of cation channels. In addition, our findings highlight the involvement of the cholinergic anti-inflammatory pathway in insult-inducible cerebellar processes. These mechanisms are likely to play similar roles in other brain regions and injuries as well, opening new venues for targeted research efforts.

Keywords: exercise ● genetic background ● glutamate ● kir6.1 ● potassium channels ● stroke

Introduction

Many neurological disorders, especially ischemic stroke [1, 2], traumatic brain injuries (TBI) and alcoholism, involve glutamatergic excitotoxicity to the cerebellum [3]. Current pharmacological agents target glutamatergic neurotransmission and secondary processes such as calcium accumulation and oxidative stress, but fail to ameliorate consequent neurological deterioration [4], sug-

gesting upstream involvement of other pathway(s). In contrast, intense physical activity (exercise) can ameliorate cerebellar damage [5] and exert protection from stroke and head injury [6, 7]. In addition, inherited variability may change one's prospects to recover from traumatic head injuries because of yet unexplained reasons [8, 9]. However, in what ways exercise and/or inherited factors affect the vulnerability to cerebellar glutamatergic damage, the underlying mechanisms and the connection between them are still not well-understood.

The protective effects of exercise on the brain were attributed by some to increased expression of neurotrophic factors, for example circulating insulin-like growth factor I (IGF-I) [5] or hippocampal BDNF [10]. Others suggested that exercise suppresses neuro-inflammation. In a rat model of stroke, exercise reduced infarct volume while preventing stroke-induced TNF-α and ICAM-1

*Correspondence to: Hermona SOREQ,
Department of Biological Chemistry,
The Hebrew University of Jerusalem,
The Edmond J. Safra Campus,
Givat Ram, 91904 Jerusalem, Israel.
Tel.: +972-2-6585109
Fax: +972-2-6520258
E-mail: soreq@cc.huji.ac.il

expression [11], and enhanced potassium influx inhibited inflamma-some formation [12]. Of note, exercise can exert either a protective or harmful effect on neurons, depending on its intensity, and the specific insult and brain structure tested. Intraperitoneal (i.p.) injection of kainic acid (kainate, 2-carboxy-4-isopropenylpyrrolidin-3-yl-acetic acid), which is a strong agonist of AMPA and kainate receptors, causes massive neuronal damage to multiple brain regions [13]. Three weeks of training on a running wheel reduced seizures induced by i.p. kainate injection [14] and 5 days training was sufficient to ameliorate kainate-dependent learning deficits, but not neuronal cell death [15]. In contrast, 30 days of voluntary training on a running wheel increased hippocampal neuronal loss exerted by local kainate microinjection in female rats [16]. Interestingly, treadmill running after cerebellar TBI in rats [17] and after cerebellar stroke in human [18] attenuated loss of Purkinje cells (PCs) and improved motor behaviour, respectively. However, to our knowledge, no one has tested the protective effect of routine exercise before cerebellar damage, and the molecular cascade underlying this effect.

AMPA and kainate receptors provide the major glutamate input to PCs, and cerebellar microinjection of kainate correspondingly causes excessive stimulation and excitotoxicity [13]. High levels of slowly desensitizing AMPA receptors [19] and calcium channels [20] make PCs especially vulnerable to ischemic stroke and glutamate excitotoxicity despite their high content of Ca^{2+}-binding proteins, such as calbindin-28K. Excessive depolarization-induced influx of Ca^{2+} through voltage-gated calcium channels, accompanied by delayed Ca^{2+} release from intracellular stores, results in disruption of axonal delivery and trafficking [21]. This depolarization leads to exaggerated vesicular release, transporter reversal or glutamate liberation after necrotic cell death, preserving harmful high levels of extracellular glutamate [3] and disrupting the cerebellar output to the rest of the brain.

Cerebellar protection may be provided by close PC interactions with Bergmann glia (BG). These cells maintain non-toxic extracellular glutamate levels, and in this way can avoid excessive glutamate uptake to PCs [3]. However, hyper-activation of glutamate receptors in BG can also damage their functioning [22]. This highlights the importance of additional neuro-protective routes, for example by inhibitory inter-neurons such as basket cells (BCs). When activated by glutamate, BCs secrete GABA to inhibit PCs, thus limiting excessive depolarization and attenuating potentially toxic consequences. BCs inhibition largely depends on anatomical structures called the 'cerebellar pinceau', which constitute BC axons wrapped around the initial segment of PC axons. The pinceau contains a rich variety of ion channels and neurotransmitter receptors, which together tightly control the emission of action potentials from PCs [23]. In addition to these potential neuroprotective structures, we predicted the involvement of acetylcholine (ACh), which acts as a modulating transmitter in the cerebellum [24], promotes survival of PCs in culture [25] and limits inflammation in the brain and periphery [26]. The goal of this study was to discover whether the cerebellar pinceau, BG or ACh, or all of them together, provide neuroprotection from acute glutamatergic stimulation to the cerebellum *in vivo*, and whether such putative protection is modulated by inherited and/or environmental input.

Materials and methods

Mouse models

Male C57BL/6 and FVB/N mice (Harlan Laboratories, Israel) were kept at the animal colony of the Herzog Hospital under standard conditions. An ethics committee of the Hebrew University in Jerusalem had approved all protocols employed in this study (IACUC #MD 112.13-3). Naive C57BL/6 mice were assigned to three groups: sedentary (SED), free access to exercise devices (EC) and treadmill-exercised (TM) mice. SED mice were kept in standard cages with no toys or exercise devices. EC mouse cages included plastic tunnels, ladders and a running wheel. Running distance was measured for each mouse, and mice that showed significantly reduced activity were omitted from the study. TM mice were subjected to routine exercise in a six-lane treadmill (model Exer-6M; Columbus Instruments, USA). On day 1, mice were habituated to the turned off apparatus for 5 min. and then to the apparatus turned on, but with unmoving belt. On subsequent days, mice ran for 5, 30 and 45 min. with the belt moving at a speed of 14 meters/min. Over the next 10 days they ran for 60 min. in a single daily exercise session. Mice that failed to walk were driven backward by the belt toward a shock-grid delivering an electric shock of 0.2–0.5 mA.

Kainate injection
Mice were anaesthetized with equithesin, a mix of pentobarbital sodium and chloral hydrate. With incisor bar set 11 mm below ear bar level, the coordinates for stereotactic microinjection (measured in mm from the lambda point) were: 1.65 posterior, 1.65 lateral and 2.2 mm ventral from skull surface. Kainate (1.0 $\mu g/\mu l$) was injected in 0.5 μl doses. Sham controls received saline in the same protocol. Operated mice were tested on a 100 cm beam-walk 9, 12 and 13 days post-operation [27]. At the end of each beam there was a cage with bedding. Once they reached the cage, mice were returned to their home cage. On days 9 and 12, mice were tested on the flat beam, which was horizontal, 3 cm wide and elevated 30 cm above floor level. On day 13, the beam had round profile with ribbed surface (for grip). Neurological evaluation involved measuring the time taken to traverse the entire length of these beams: the more deficits, the longer it took for a mouse to complete a walk.

Immunohistochemistry

Tissue preparation and staining
See 'Supplementary Methods' in Supporting Information.

Analysis of histological data
Lesion size was estimated by measuring cross-section areas in sagittal sections stained with cresyl violet. Axonal beading was quantified in sagittal sections stained with mouse antibody against calbindin D28k, using the 'analySIS' software (Soft Imaging System GmbH, Munster, Germany). Beads were counted in one lobule located at the penumbra of the lesion. Axonal width was measured in the same sections using the Image-pro software (Media Cybernetics, MD, USA). Fifty axons were measured in each image, and 13–27 images were analysed for each treatment group. For semi-quantification of HCN1 and KVβ2 immuno-staining, at least three sagittal cerebellar sections were sampled from each hemi-cerebellum of each mouse. The three anterior lobules were sampled from each section.

Using the 'analySIS' image analysis software, the layer where pinceau structures appear was encircled and the percent of immunostained area was calculated. Semi-quantification of Kir6.1 was similar, but here we looked at the PC and molecular layers instead of the pinceau region, and used the public domain, JAVA-based ImageJ software.

RT-PCR arrays

RNA extraction

Sham and kainate-injected sedentary and exercised mice were sacrificed 24-hr post-injection, the right side of the cerebellum was dissected and RNA was extracted using the RNeasy lipid tissues minikit (Qiagen, Hilden, Germany). Eight hundred nanograms of total RNA were reverse transcribed (RT) in 20 μl reaction mixtures using the RT^2 First Strand Kit (Superarray, MD, USA). Real time PCR was performed using the 'Mouse Neuroscience Ion Channels & Transporters PCR Array' and 'RT^2 Real-Timer SyBR Green/ROX PCR Mix' (Superarray) on an ABI Prism 7900 Sequence Detector (Applied Biosystems, CA, USA) according to the manufacturer's instructions.

Data analysis

PCR 'threshold cycle values (C_Ts)', as indicated by the sequence detection system (SDS) software, were used for calculation of expression values. These values were further normalized using a combination of four different house keeping genes and were used for the following analysis: (1) unsupervised hierarchical clustering of gene expression profiles which is presented as a dendrogram and a colour map based on a threshold of 3.2 for better visualization of the expression profiles. Clustering was made on a complete data set. (2) Principal component analysis (PCA) and clustering using K-means algorithm. K-means clustering results are presented as points connected to the group mean. Distinction was measured as the ratio of the sum of distances between group's points and their mean, and sum of distances between all points and the global mean (thus, low ratio indicates high distinction). The ratio of the presented graph was 0.475 and its significance was calculated to be 0.025 using 300 samples permutations. (3) One-way ANOVA, *post hoc* analysis and Spearman's correlation test for identifying transcripts that were affected by kainate injection in an exercise-modulated manner. The 'sham-sedentary' group was referred to as control, and the other treatment groups (kainate-sedentary, kainate-exercise) were individually compared with this group. Therefore, fold-change for each gene was calculated as difference in transcript levels between the control and one of the experimental groups. These values were transformed to a log scale for better visualization. Positive values indicate up-regulation and negative values indicate down-regulation.

Acetylcholinesterase enzyme activity measurements and Real-time RT-PCR for quantifying cytokines expression

See 'Supplementary Methods' in Supporting Information.

Evaluation of Purkinje cell degeneration in live cerebellar slices

FVBN mice (3 months old) were deeply anaesthetized with pentobarbital sodium (over 40 mg/kg body weight) and were perfused by intracardial injection of physiological ice-cold sucrose solution (5 mM KCl, 1.9 mM MgSO$_4$, 1.25 mM KH$_2$PO$_4$, 26 mM NaHCO$_3$, 11 mM glucose, 2.7 mM CaCl$_2$, 125 mM sucrose) until the face and extremities became pale. The head was quickly severed, the brain exposed and the cerebellum sepa-

rated. After 30 sec. in oxygenated (5% CO$_2$) ice-cold sucrose physiological solution, the cerebellum was para-sagitally cut to 300-μm-thick slices in the same ice-cold solution using a Leica VT1000S slicer. Slices were incubated (20 min., in sucrose physiological solution, room temperature) and then the solution was slowly (within 1 hr) replaced by normal oxygenated (5% CO$_2$) physiological solution (124 mM NaCl, 5 mM KCl, 1.3 mM MgSO$_4$, 1.2 mM KH$_2$PO$_4$, 26 mM NaHCO$_3$, 10 mM glucose, 2.4 mM CaCl$_2$). Slices were randomly divided into treatment groups and were incubated for 20 min. either in normal physiological solution or with physiological solution containing 20 or 100 nM glibenclamide or 0.5% Dimethyl sulfoxide (DMSO). Then, they were placed in either normal physiological solution or 20 μM kainate for 30 min., and finally were all transferred to normal physiological solution for an additional period of 5.5 hrs. Then, slices were fixed by immersing in 4% paraformaldehyde, 4% sucrose phosphate buffer solution for 24 hrs and then in 12% sucrose phosphate buffer solution for several days.

Fluorojade (FJB) staining and quantification

Slices were glued to a cryostat stage, cut at 18 μm intervals, mounted on SuperFrost Plus slides (Thermo-Fisher Scientific, Meiningen-Dreissigacker, Germany), dried at room temperature for 1 hr and kept in a cryopreservation buffer (similar to that used for immunohistochemistry) at -18°C until staining. Before staining, slides were rinsed in saline 5 min., then in ascending concentrations of alcohol – 70%, 90% and 100%, 3 min. each and then rehydrated and processed for FJB staining. Briefly, slides were treated with potassium permanganate (15 min.) for reducing non-specific staining, rinsed in saline, slides sections were laid on them horizontally and covered with 250 μl of FJB staining solution (0.0005% FJB in 0.1% acetic acid solution in saline) and a piece of parafilm for 30 min. at room temperature. The reaction was stopped by rinsing in saline. Sections were then counterstained with the fluorescent Nissl stain DAPI, dried at room temperature and then cover-slipped in Immumount (Shandon, Pittsburgh, PA, USA). Measured FJB staining intensities of PCs were normalized to background intensity using ImageJ software. Approximately 15–30 cells were quantified in each section.

Statistical analysis

In all bar graphs, bars represent means $\pm$ standard evaluation of mean (S.E.M.). Means of two samples were compared using either Student's *t*-test or Mann–Whitney (MW) test, as indicated. Means of more than two samples were compared using 1- or 2-way(s) ANOVA followed by appropriate *post hoc* analysis. Histograms were compared using Kolmogorov–Smirnov test. For details see Supporting Information. Spearman's correlation test and PCA analysis were also employed in array analysis. Array data analysis was performed by Matlab (Mathwork, MA, USA) and SPSS (SPSS, IL, USA) software. All other analyses employed Excel, Statistica (Statsoft, OK, USA) and Prism (GraphPad, CA, USA) software.

Results

To study the effects of exercise and genetic background on coping with acute kainate-induced damage to the cerebellum, we compared cerebellar damage in sedentary and exercised C57BL/6, and in FVB/N mice. We have identified ion channels that

play a role in the susceptibility of PCs to kainate toxicity, mapped the changes in their expression to the pinceau and BG, and manipulated cerebellar slices to avoid such changes. We also searched for cholinergic modulations that may relate to post-kainate neuro-inflammation.

Both exercise and genetic background protect Purkinje cells from kainate damages

Inbred C57BL/6 mice were exposed to cerebellar microinjection of kainate or saline and examined after 14 days of sedentary, free exercise (EC) or forced treadmill training (TM) conditions. To explore the role of genetic background in the susceptibility to kainate, we also examined sedentary FVB/N mice, which are known to be more vulnerable than C57BL/6 mice to the toxicity of systemically injected kainate [28].

As in stroke, each lesion had a 'core', namely a spherical region forming around the injection site, and a 'penumbra', a peripheral surrounding region in which depolarization or excessive glutamate release can occur long after kainate microinjection [4]. Neither exercise nor genetic background had an effect on the core region diameter ($n = 5–9$ per group, $P = 0.45$ and 0.26, respectively, Student's t-test, Fig. S1A) In contrast, we found clear differences in the number of calbindin-28K-positive axonal beads, focal pathological swellings characteristic of diverse neuronal malfunctions including ischemic stroke [29], in the penumbra (Fig. 1A-i). In sedentary C57BL/6 mice, kainate injection predictably increased bead counts in PCs ($n = 5–15$ per group, $P = 0.00014$, post hoc analysis after two-way ANOVA). However, either free or enforced exercise preceding the injections attenuated axonal beading compared to sedentary mice, suggesting that exercise confers cerebellar protection from subsequent kainate damage ($n = 5–15$ per group, $P = 0.00022$ or 0.00016, respectively, post hoc analysis after two-way ANOVA, Fig. 1A-ii). Similar trends were seen 1 day post-injection ($n = 3–6$, Fig. S1B). Importantly, 'forced-training' on a treadmill and 'voluntary activity' on a running wheel conferred a similar level of protection. Surprisingly, axonal pathology was more severe in kainate-injected C57BL/6 than in FVB/N mice ($n = 5–15$ per group, $P = 0.0012$, Student's t-test, Fig. 1A-ii). Moreover, C57BL/6 axon diameter, which can also indicate neuronal pathology [30] was generally larger in C57BL/6 than in FVB/N-injected mice; and exercise before kainate injection attenuated this difference ($n = 5–15$ per group, $P < 0.0001$,
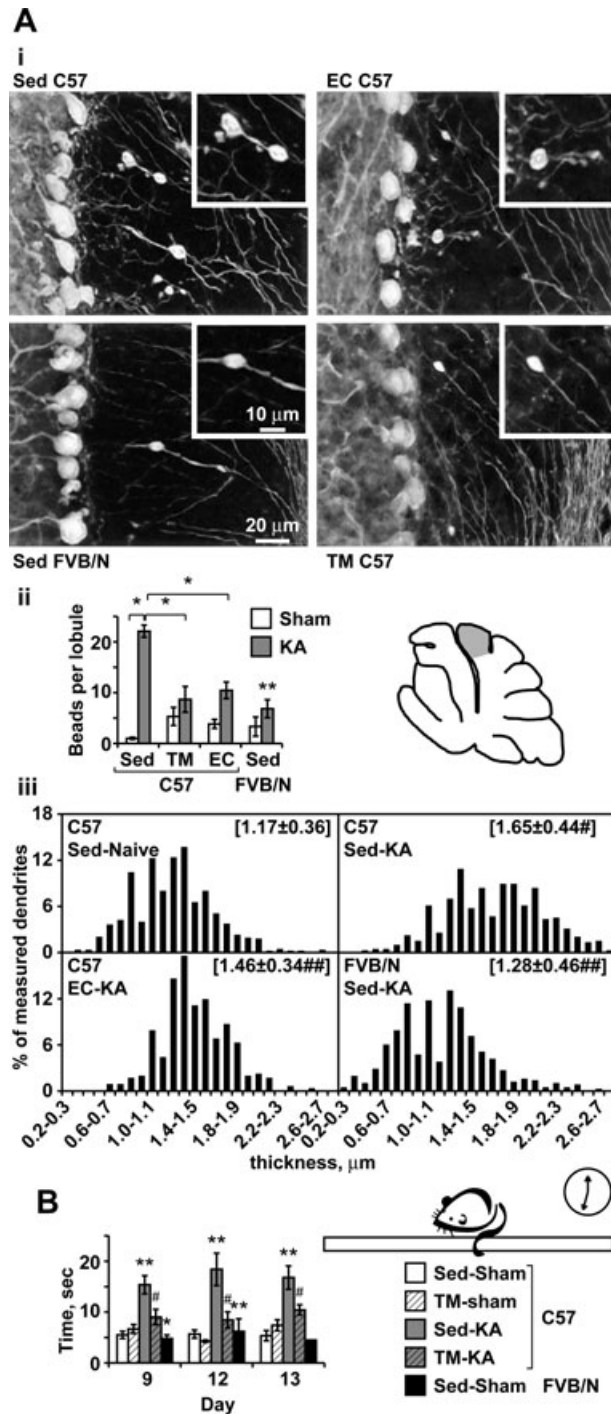
Fig. 1 Exercise and genetic background affect cerebellar vulnerability to kainite. (**A**) Axonal beading and swelling after kainate injection is reduced in exercised C57BL/6 (C57) and FVB/N mice. Shown is calbindin-28K staining (I), bead counts (II) and axonal width (III) in cerebellar sections dissected 14 days post-injection with kainate of sedentary (SED), free exercise (EC) and treadmill trained (TM) C57BL/6 mice, and sedentary FVB/N mice. Scheme: the cerebellar area (lobule) used for bead counts (KA: kainite; sham: saline injection; $n = 5–15$ per group; *$P < 0.0005$, post hoc analysis after two-way ANOVA; **$P < 0.0005$ in comparison to kainate-treated sedentary C57BL/6 mice, Mann–Whitney test; #$P < 0.0001$ in comparison to C57BL/6 Sed-Naïve, ##$P < 0.0001$ in comparison to C57BL/6 Sed-KA, Kolmogorov–Smirnov test). (**B**) Improved 'beam-walk' performance of exercised C57BL/6 and sedentary FVB/N mice after kainate injection. Shown is the time in minute to complete a walk on the beam ($n = 5–11$ per group, *$P < 0.05$, **$P < 0.005$ in comparison to Sedentary-Sham C57BL/6 mice, #$P < 0.05$ in comparison to sedentary-kainate C57BL/6 mice; post-hoc analysis after two-way ANOVA).

Fig. 2 Cerebellar ion channels participate in the exercise-modulated kainate response. (**A**) Analysis of real-time PCR array data. Upper: Unsupervised hierarchical clustering (dendrogram) of transcript expression profiles. The *Y*-axis shows proximity values (Euclidian distance). Note classification into the four treatment groups, with one misclassified mouse (top asterisk). Lower: expression matrix of those transcripts used for hierarchical clustering. Rows = transcripts, columns = individual mice. Expression values are colour coded. (SS: sedentary-sham; ES: exercised-sham; SK: sedentary-kainate; EK: exercised-kainate). (**B**) PCA of the array data differentiates between the four treatment groups. Presented is a scatter plot in the PC2/PC4 plane, which is the combination that yields maximal distinction between groups. Each mouse is indicated by a single point, coloured as in the dendogram. Distinction ratio = 0.475 ($P = 0.025$, see Materials and methods section for detailed explanation). (**C**) Kainate-inducible, exercise-preventable changes. Out of 79 genes in the array, the expression levels of seven genes were changed in this manner ($n = 6$ per group, *$P < 0.05$ Tukey's *post-hoc* analysis after one-way ANOVA).Three of these genes showed changes significantly correlated with the neurological score ($P < 0.001$, Spearman's correlation test). Left and middle columns show fold- changes of transcript expression level (in a logarithmic scale shown on the left side). Right column: correlation coefficients between transcript expression levels and mouse 'neuronal score' (Table 1, colour scale in the right side). White boxes note insignificant values.
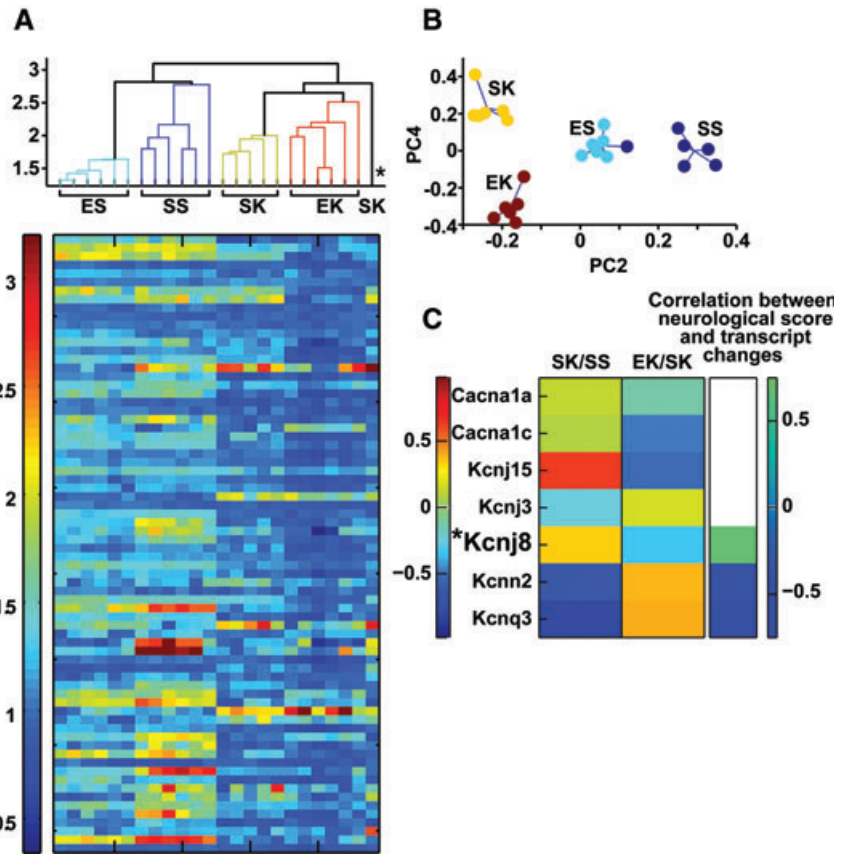
Kolmogorov–Smirnov test, Fig. 1A-iii). At the behavioural level, exercise improved the performance of kainate-injected mice in a beam walk test 9, 12 and 13 days post-treatment. Kainate-injected FVB/N mice showed better performance than C57BL/6 mice in this test at all time points ($n = 5$–11 per group, $P < 0.05$, *post hoc* analysis after two-way ANOVA, Fig. 1B), again demonstrating innate protection. Thus, both genetic background and exercise appeared to affect susceptibilities to kainate damage, and these differences were reflected in axonal pathologies as well as in the post-injection neurological score.

Inward rectifying potassium channels mediate cerebellar protective effects

Because intra- and extracellular ionic concentrations determine the physiological activity of PCs, we predicted that exercise-inducible and/or inherited differences in the expression of ion channels in BG, BCs and other PCs-interacting cells might protect the cerebellum from glutamate excitotoxicity. Therefore, we injected sedentary and exercised mice with either kainate or saline and measured the

cerebellar expression of 79 different ion channel transcripts 1 day post-injection by real-time PCR array. We then searched for cerebellar ion channels whose mRNA expression levels were altered by kainate, but these changes were prevented or attenuated by previous exercise (see Supporting Information for complete raw data and Fig. S2 for visualization of expression changes in all transcripts on the array). Apparently, ion channels are strongly affected by both kainate injection and exercise. Therefore, different treatment groups (Sham- *versus* kainate-injected mice, with/without preceding exercise) demonstrated distinct patterns of ion channel transcripts and unsupervised hierarchical clustering of the expression data correctly classified all but one of the mice into their different groups. Importantly, the misclassified animal was not falsely attributed to any other treatment group (Fig. 2A). PCA further demonstrated the clustering into treatment groups. However, exercised, kainate-injected (EK) mice were distinct from sedentary, kainate-injected (SK) mice, but are not significantly closer to exercised (ES) and sedentary (SS) sham-injected mice, suggesting that when examining the expression of ion channels as a group; preceding exercise alters the expression pattern after kainate injection, but not by making it similar to sham-injected mice (Fig. 2B).

Table 1 Neurological evaluation at 24-hr post-injection

Score	Performance description	N for each score*
1	Normal	6-Sedentary sham, 6-EC sham, 0-Sedentary KA, 1-EC KA
2	Walking upright but ataxic	0-Sedentary sham, 0-EC sham, 2-Sedentary KA, 4-EC KA
3	Walking upright, ataxic and maintaining contact of the right shoulder and torso (which is ipsilateral to the lesion) with the cage wall	0-Sedentary sham, 0-EC sham, 0-Sedentary KA, 0-EC KA
4	Lateropulsion (rolling over toward the side of the lesion)	0-Sedentary sham, 0-EC sham, 1-Sedentary KA, 1-EC KA
5	Lying on the side ipsilateral to the lesion with or without limb movements but respiration was normal	0-Sedentary sham, 0-EC sham 3-Sedentary KA, 0-EC KA
6	Lying on the side ipsilateral to the lesion, inactive and with respiration heavy or irregular	0-Sedentary sham, 0-EC sham, 0-Sedentary KA, 0-EC KA

*Number of mice achieving this score (out of 6) in each treatment group.

Prominent kainate-induced changes occurred in 49 of these tested transcripts, but only seven were inversely affected by pre-injection exercise ($n = 6$ per group, Fig. 2C, $P < 0.05$, *post hoc* analysis after one-way ANOVA). Three (42.9%) of these genes (KCNJ8, KCNN2 and KCNQ3) were inward-rectifying potassium channels, which constituted only 8.9% of the total transcripts on the array. This number is higher than expected by chance ($P = 0.012$, hypergeometric distribution). Three of the seven identified genes further presented a significant correlation between transcript levels and the post-injection neurological scores ($P < 0.001$, Spearman's correlation test, Fig. 2C, see Table 1 for details of the neurological assessment scale and the scores for each treatment group). Specifically, KCNJ8 mRNA transcripts encoding the Kir6.1 protein were significantly up-regulated by kainate injection to sedentary mice, but down-regulated by kainate administration after exercise. Moreover, KCNJ8 expression levels were significantly correlated with the neurological score of each mouse.

Kir6.1 over-production protects cerbellar neurons from Kainate damage

Kir6 proteins constitute the pore-forming subunit of K-ATP channels. Together with a regulatory sulfonylurea receptor (SUR1 or SUR2), they form ATP-dependent inward rectifying potassium channels. Kir6.1 activation associates with reduced extracellular glutamate, presumably because of altered glutamate uptake by either neurons or glia [31–33]. Therefore, we chose Kir6.1 for fur-

ther exploration and tested the spatial nature of the observed changes and their physiological relevance.

First, we examined changes in Kir6.1 protein levels at a later time point. After the induction of Kir6.1 transcription 1 day post-kainate injection, Kir6.1 protein levels returned to those seen in control C57BL/6 mice within 14 days ($n = 6$–9 per group, Fig. S3), reflecting the transient nature of the induced changes. The transient transcriptional induction by kainate could be either a marker of cell damage, or a beneficial protection mechanism. Therefore, we tested basal Kir6.1 protein levels in the more resist-ant, namely exercised C57BL/6 or sedentary FVB/N mice. Exercise significantly enhanced Kir6.1 labelling in BG of sedentary naïve mice. Similarly, in FVB/N, the basal levels of Kir6.1 were higher compared to those of C57BL/6 mice ($n = 6$–9, $P < 0.005$, Student's *t*-test, Fig. 3A), Thus, higher levels of Kir6.1 protein expression in BG were correlated with improved resistance to kainate in non-injected mice.

To test whether Kir6.1 expression actively contributes to the enhanced cerebellar resistance to kainate, and not just correlates with it, we treated live cerebellar slices with the SUR1 antagonist, glibenclamide and examined the effect of blocking SUR1-Kir channels on kainate-mediated damage to the cerebellum. We chose the relatively resistant FVB/N mice for this experiment to enable better visualization of the predicted enhancement in cell death exerted by glibenclamide. Slices were pre-treated with glibenclamide and then exposed to kainate and degenerating neurons were quantified by Flourojade staining. Kainate exposure enhanced neuronal degeneration (two-way ANOVA: main effect of kainate: $P < 0.0001$),

Fig 3 Kir6.1 channel protects the cerebellum from kainate damage. (**A**) Cerebellar Kir6.1 levels. Both types of exercise (EC and TM) significantly enhanced Kir6.1 expression, and the basal Kir6.1 levels were higher in FVB/N than C57BL/6 (C57) mice (semi-quantification is based on percentage of Kir6.1 immunoreactive stained area, control value is 3.6%, $*P < 0.0005$, *post-hoc* analysis after one-way ANOVA, $^\#P < 0.005$ in comparison to sedentary C57BL/6 mice, Student's *t*-test, $n = 6$–9 per group). (**B**) Glibenclamide augments Kainate damage. Sagittal cerebellar slices were treated for 20 min. with either DMSO or glibenclamide (gli, 20 nM) and then with or without 20 μM kainate (30 min.). Shown are Purkinje cells stained with Flurojade B 5.5 hrs after treatment. Top: Semi-quantification is based on staining intensities normalized to background staining, as measured by Image J and control value of 95.1 arbitrary units, $n = 4$–8 mice per treatment group, $*P < 0.0005$ in comparison to naïve mice, *post-hoc* analysis after two-way ANOVA. Bottom: Distribution histograms of Flurojade B staining intensity in each treatment group. The distributions are significantly distinct from each other ($P < 0.05$, Kolmogorov–Smirnov test, a.u.: arbitrary units). Note enhanced neuronal degeneration after kainate injection, and its augmentation by glibenclamide pre-treatment.
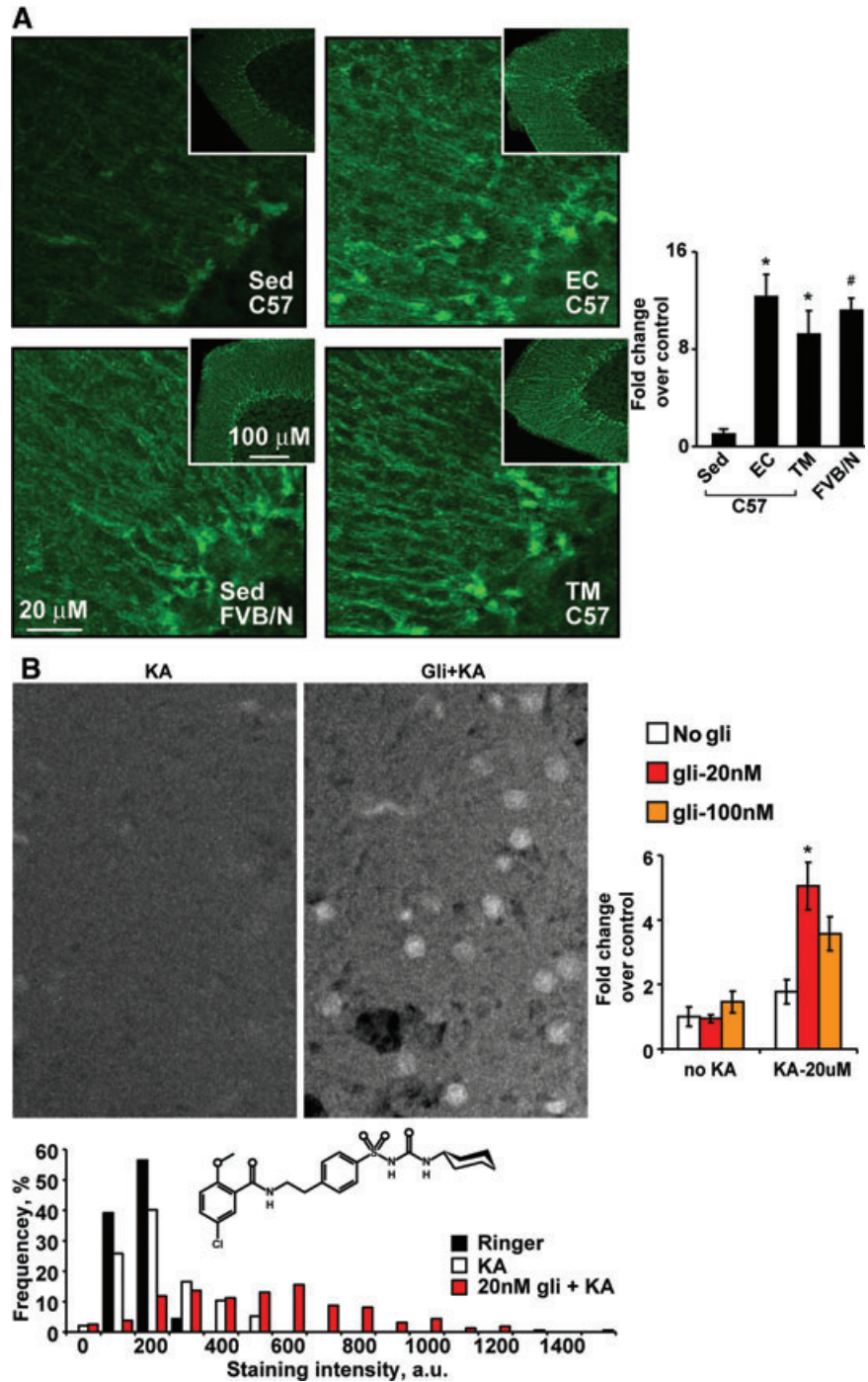
and glibenclamide pre-treatment further aggravated neuronal cell death (two-way ANOVA: main effect of glibenclamide: $P = 0.03$). Twenty nanometres of glibenclamide had a stronger effect than 100 nM ($n = 4$–8 per group, $P < 0.001$, *post hoc* analysis, Fig. 3B, top), possibly reflecting opposing effects on other glibenclamide-sensitive Kir6 channels that is exerted by higher levels of

this agent. Distribution analysis of FJB staining intensities highlighted the induction of neuronal degeneration by kainate treatment ($P = 0.045$, Kolmogorov–Smirnov test), and its enhancement by pre-treatment with either 20 or 100 nM glibenclamide ($P < 0.000001$, Kolmogorov–Smirnov test) (Fig. 3B, bottom and Fig. S4). That Kir6 inhibition negated the neuronal
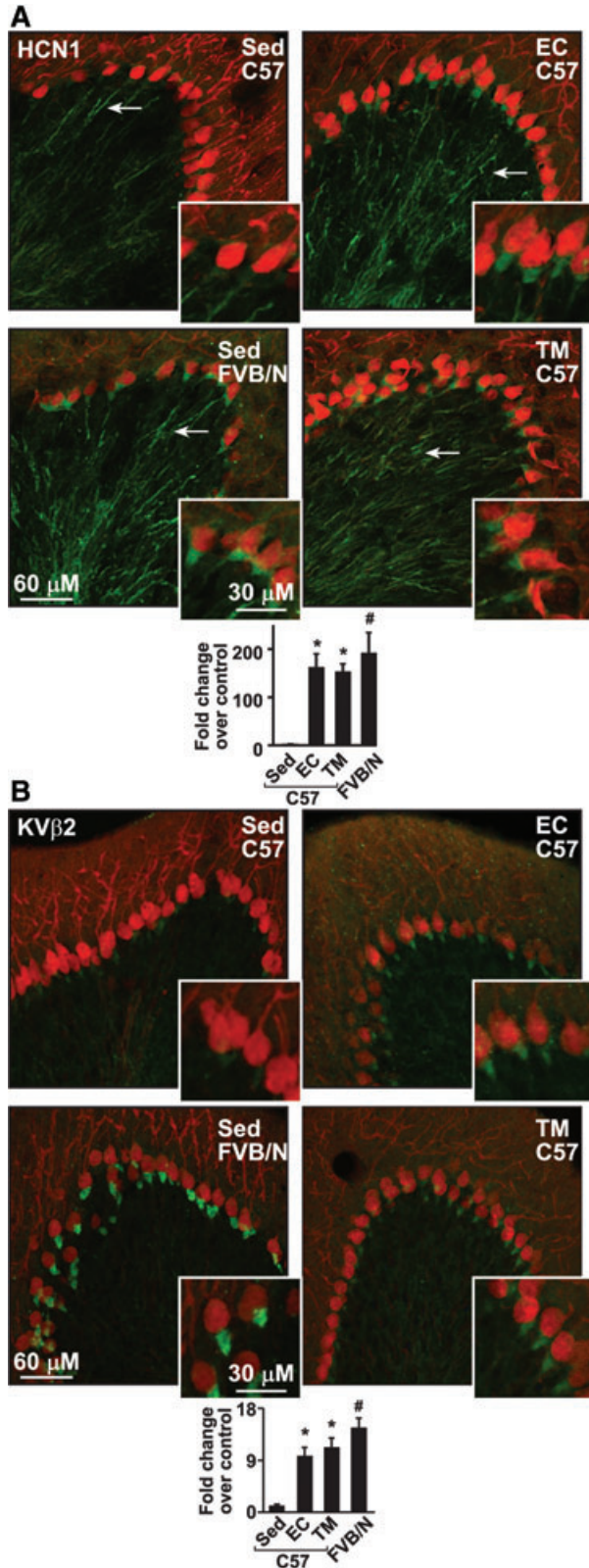
Fig. 4 Higher HCN1 and KVβ2 levels in the cerebellar pinceau of protected mice. Labelling of HCN1 (**A**) and KVβ2 (**B**) in the cerebellar pinceau of kainate-injected and exercised C57BL/6 and sedentary FVB/N mice, which show higher resistance to glutamatergic toxicity (green = HCN1 or KVβ2, red = calbindin-28K, $n = 6$ for each group, insets show the pinceau region). Semi-quantification is based on percentage of HCN1 and KVβ2 immunoreactive stained areas. Control values were 0.04% and 0.4%, respectively. (*$P < 0.0005$ in comparison to sedentary C57BL/6 mice, *post-hoc* analysis after one-way ANOVA, #$P < 0.005$ in comparison to sedentary C57BL/6 mice, Student's *t*-test. Arrows indicate staining outside the pinceau).

protective effect of its high-level expression suggests that the ion channel properties of Kir6.1 are causally involved in this effect.

Up-regulated potassium channels accumulate in the cerebellar pinceau

We surmised that in addition to BG, other neighbouring structures protect PCs from glutamate excito-toxicity. Specifically, we suspected the pinceau region of BCs. To challenge this prediction, we examined the expression levels of four voltage-dependent channels that are highly prevalent in the pinceau, namely HCN1, KVβ2, KV1.2 and the γ-amino butyric acid (GABA) transporter—GAT1A. The cerebellar pinceau of exercised C57BL/6 and sedentary FVB/N mice, both relatively resistant to kainate, showed higher levels than sedentary C57BL/6 mice of both HCN1 ($n = 6$ per group, $P < 0.0005$ and 0.0083, respectively, Fig. 4A) and KVβ2 ($n = 6$ per group, $P < 0.0005$ and 0.00045, respectively, Fig. 4B). Interestingly, HCN1 but not KVβ2 staining could also be seen outside the pinceau (Fig. 4A, white arrows). Thus, resistance to glutamate toxicity correlated with elevated expression levels of both HCN1 and KVβ2 in the pinceau and of Kir6.1 in BG.

Exercise-induced cholinergic fibres associate with suppressed cerebellar cytokines

ACh modulates glutamate signalling in some, but not all PCs. There is still a debate whether its effect is excitatory or inhibitory and what are the responsible mechanism(s) [24, 34]. In addition, ACh may limit the production of pro-inflammatory cytokines and in this way attenuate the activation of their receptors on PCs, affecting calcium accumulation and neuronal firing [35–37]. For these reasons, we aimed to explore exercise-mediated changes in cholinergic signaling that may be involved in its protective effect. BG showed high levels of α7nAChR mRNA, but these were not altered by exercise ($n = 4$–6 per group, $P > 0.05$, MW test, Fig. 5A). However, acetylcholinesterase (AChE) activity staining demonstrated an increased number of AChE-positive 'varicosities' in neuronal fibres [38] of exercised mice, probably reflecting more ACh release sites ($n = 4$–6 per group, $P < 0.05$, MW test, Fig. 5B). In contrast, we did not detect significant exercise-inducible AChE

activity changes in cerebellar homogenates (n = 5–8, P > 0.05, MW test, Fig. 5C), indicating that exercise-induced cholinergic changes are limited to specific neuronal structures. Of note, we further showed significant exercise-induced reduction of AChE activity in the serum (n = 5–8, Fig. 5C, P < 0.05, MW test), suggesting enhanced systemic control of inflammation.

Both ischemic stroke in human patients [39] and kainate injection in mice [40] increase the expression of pro-inflammatory genes in the brain, inversely to the predicted effect of ACh. Correspondingly, quantitative RT-PCR demonstrated kainate-mediated increases in the transcript levels of the cerebellar pro-inflammatory cytokines, IL-6 and TNF-α and the chemokines, MCP-1 (CCL2) and KC (CXCL1) (n = 6 per group, P < 0.0005, *post hoc* analysis after two-way ANOVA). In non-injected mice, exercise had no effect on cytokine levels, but preceding exercise attenuated the kainate-induced cerebellar increases in three of the four transcripts (n = 6 per group, P < 0.05, *post hoc* analysis after two ways ANOVA, Fig. 5D). Thus, cerebellar cytokine production is inversely related to the exercise-inducible increase in cerebellar cholinergic release sites and directly related to circulating AChE levels, supporting the notion that exercise enhances cholinergic signaling and suppresses the damaging outcome of inflammation in the cerebellum.

Discussion

We found that convergent innate and exercise-inducible factors protect the micro-environment of PCs from glutamate excito-toxicity characteristic of stroke and other brain injuries. BG and BCs showed increased expression of the ATP-dependent potassium channel, Kir6.1, and in HCN1 and KVβ2 channels, respectively. Blocking ATP-dependent potassium channels increased the kainate-induced damage in cerebellar slices, further indicating a causative, rather then correlative, role for Kir6.1 abundance in cerebellar protection from glutamate toxicity. Kir6.1 potentially optimizes energy maintenance in PCs by the adjacent BG, whereas HCN1 and KVβ2 potentiate the inhibitory signals sent from BCs to PCs at the cerebellar pinceau. Exercise further enhanced the cholinergic input to the cerebellum and in the circulation, likely modifying PCs firing patterns and facilitating the cholinergic anti-inflammatory effect in the brain and periphery.

Our study confronts several methodological concerns. First, it is possible that the protective effect of exercise is indirect, because of prevention of metabolic, hypertension and/or cardiovascular impairments [6]. However, we employed healthy young adult
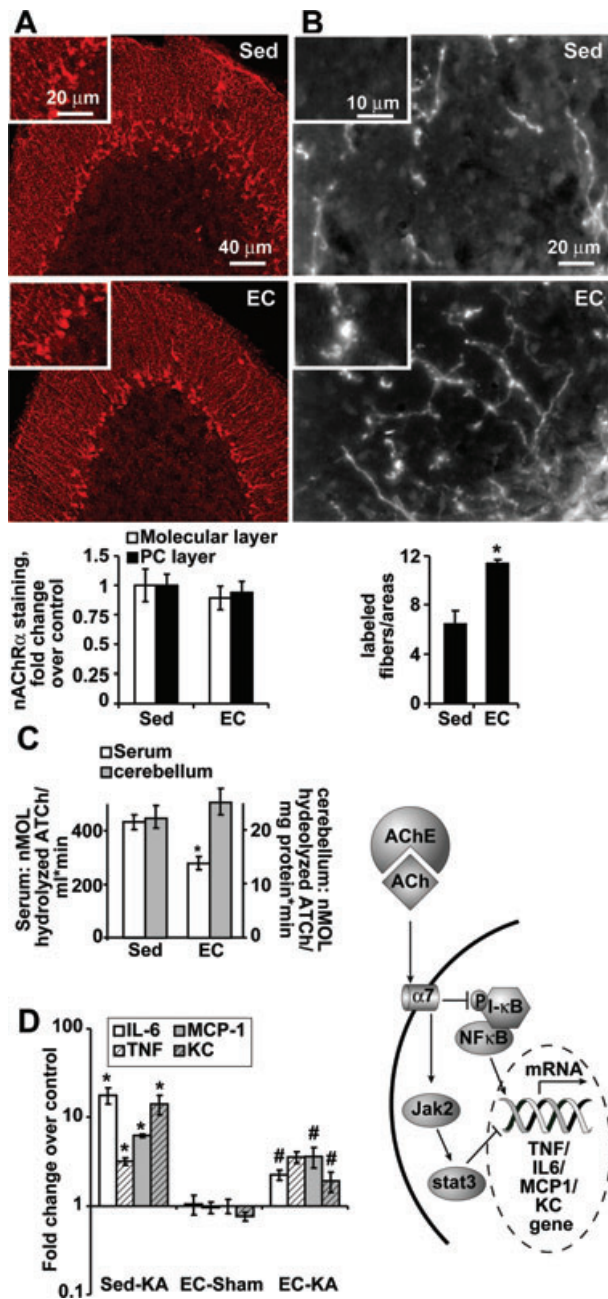

Fig. 5 Exercise modulates the cerebellar cholinergic system. (**A**) BG cells express similar levels of α7 nicotinic receptor in sedentary and exercised C57BL/6 mice (n = 4–6 per group, P > 0.05, Mann–Whitney test). (**B**) Cholinergic release sites as indicated by Karnovsky staining in cerebellar sections (axonal varicosities, n = 4–6 per group, *P < 0.05, Mann–Whitney test). (**C**) Ellman's assay show a significant decrease in AChE activity in the periphery (serum, n = 5–8 per group, *P < 0.05 in comparison to Sed, Mann–Whitney test), but not in the cerebellum. (**D**) ACh inhibits expression of pro-inflammatory cytokines in the circulation (right). Correspondingly, preceding exercise attenuates kainate-mediated elevation in cerebellar transcript levels of the noted pro-inflammatory cytokines and chemokine (left, n = 6 per group, *P < 0.0005 in comparison to sedentary-sham, #P < 0.05 in comparison to Sedentary kainate, *post hoc* analysis after two-way ANOVA).
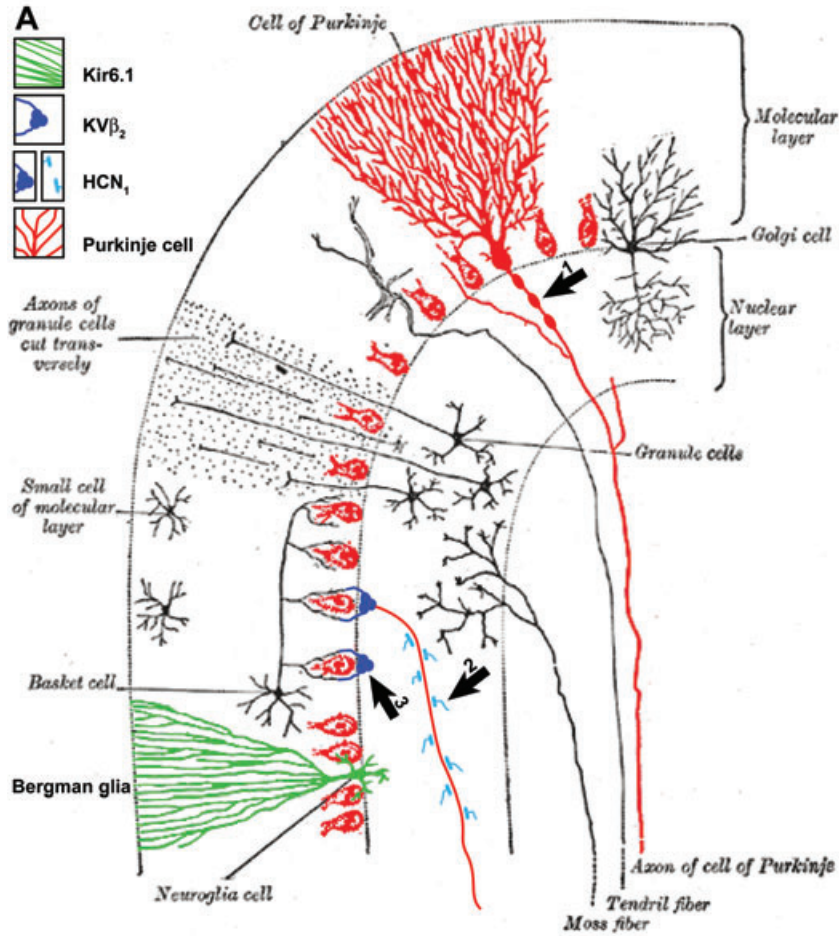
Fig. 6 Potential molecular mechanisms underlying increased resistance to glutamatergic excitotoxicity. (**A**) Enhanced expression of Kir6.1 in BG, and HCN1 and KVβ2 in BCs, is associated with reduced damage to the axons of adjacent Purkinje cells after kainate injection. (1) beads on the axon of Purkinje cell (2) HCN1 staining in the vicinity of Purkinje cells axons (3). HCN1 and KVβ2 staining in the pinceau of BCs. (**B**) Protected mice (exercised C57BL/6 or sedentary FVB/N) show higher levels of HCN1 and KVβ2 in the cerebellar pinceau, higher levels of Kir6.1 in BG and lower levels of pro-inflammatory cytokines, preventing inflammation-mediated neuronal damage (right). In contrast, vulnerable mice (sedentary C57BL/6) show lower HCN1 and KVβ2 labelling in BCs and lower Kir6.1 levels in BG. Purkinje cells in the vulnerable mice are also exposed to higher levels of pro-inflammatory cytokines (left). The axons of these cells have more beads, indicating stronger damage exerted by Kainate injection. In contrast, vulnerable and protected mice have similar levels of α7 nicotinic receptors.
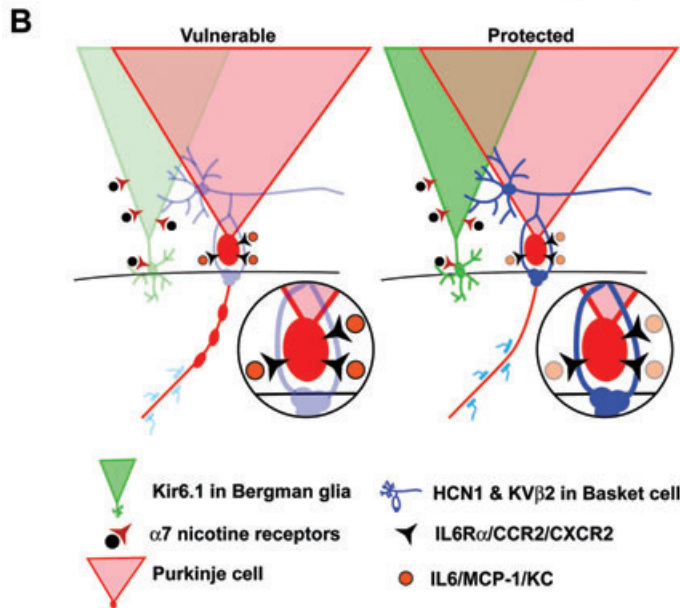
mice, and a relatively short period of physical training supporting a direct protection by attenuation of focal glutamate toxicity. Secondly, 'forced-training' treadmill running and 'voluntary activity' of free access to a running wheel similarly up-regulated potassium channels expression and protected trained animals from neurological deficits. This generalizes the implications of our study beyond the enriched environment supplied by the running wheel or the stress induced by daily forced training to a broad effect of physical activity. Thirdly, it is possible that exercise alters the bio-availability (*e.g.* uptake, stability or clearance) of kainate rather than attenuating its debilitating effect. Moreover, it is possible that the consequences of exercise depend not only on its intensity and duration, but also on its timing relative to the injury.

Kir6.1 channels are ATP-dependent potassium channels, activated by low cytoplasmatic ATP concentrations and therefore couple the metabolic state of the cell with its electrical activity [31]. Kir6.1-encoding transcripts were modestly but significantly increased 24 hrs post-kainate injection, an effect which was avoided after exercise. Given that sedentary FVB/N and exercised C57BL/6 mice showed higher Kir6.1 levels than the more vulnerable sedentary C57BL/6 mice, we postulated that Kir6.1 is protective rather than detrimental. Elevated Kir6.1 levels in cerebellar BG [41] can potentially preserve normal cellular functioning under toxicity-mediated depletion of ATP and prevent changes in membrane potential. This avoids the reversal of glial glutamate transporters after ATP depletion and normalizes potassium outflow, limiting the firing rate of PCs [42]. For example, in a mouse model of tuberous sclerosis, astrocytic Kir6.1 contributed to protection from neuronal hyperexcitability [33]. In this way, exercise may 'train' the cerebellum to anticipate and cope with changes in ATP availability and metabolic stress, two characteristic hallmarks of glutamate over-excitation. When the innate Kir6.1 levels are low, rapid exposure-induced increases in KCNJ8 transcripts may improve coping with glutamatergic insults; but in exercised mice, where Kir6.1 protein levels are already high, such accelerated transcription is unnecessary. Exercise- and kainate-mediated increases in Kir6.1 proteins and/or transcripts can thus reflect a-priory anticipation of, or post-factum response to insults, respectively. Tracing mutations in the Kir6.1 gene will show if it protects from stroke, traumatic brain injury and alcoholism and if that is the case, carriers of debilitating mutations in this gene should be strongly advised to incorporate daily exercise into their routine.

In cerebellar slices from the apparently resilient FVB/N mice, glibenclamide blockade of SUR1-regulated channels aggravated kainate-inducible neuronal damage. Glibenclamide also blocks Kir6.2-SUR1 channels, which are prevalent in PCs and other cerebellar neurons [41] but were not changed under kainate and/or exercise. Previous studies showed contradicting results by demonstrating protective effects for glibenclamide in rodent models of stroke [43], although one study showed a negative post-stroke effect of this agent [44]. SUR1 can bind and regulate both Kir6.1 and Kir6.2 channels, and was recently found to control also ATP-dependent, non-selective cation channels [43]. Therefore, these contradicting effects of glibenclamide may reflect brain region differences in the concentration of these different SUR1-

controlled channels [41]. Alternatively, or in addition, systemic administration of Kir channel blockers can protect the brain because of blocking Kir channels in the periphery. In rats, the ATP-dependent potassium channels opener, Iptakalim, improves glutamate uptake both in cultured neurons [32] and glia [45], and protects against hypoxic brain damage [44]. Further studies of Kir6 channel modulators are required to assess their potential prophylactic value under high risk of ischemic stroke, and as post-event therapies of stroke, traumatic head injury and alcoholism.

Screening of cerebellar ion channel candidates revealed kainate-inducible and exercise-preventable change in the expression of inward rectifying potassium channels as a group, suggesting that additional cerebellar potassium channels might be involved. Accordingly, both exercise and inherited protection up-regulated two voltage-dependent cation channels in the pinceau, Kvβ2 and HCN1, compared to sedentary C57BL/6 mice. The β subunits of voltage-dependent potassium channels (KVβs) are auxiliary units that assemble with KV1 or KV4 α subunits to form heteromeric KV channels and increase their kinetics, localization and expression [46]. In the cerebellar pinceau, BCs secrete GABA, generating a strong inhibitory effect on the soma and on the initial axon segment of PCs. Therefore, enhanced expression of KVβ2 may increase the activity of KV1 and KV4 channels, contributing to a yet more efficient inhibitory input to PCs. HCN channels carry an inward rectifying 'hyper-polarization-activated current (I_h)' produced by influx of Na^+ and K^+ ions [47] and are activated by hyper-polarization and deactivated by depolarization. Given that they participate in maintaining the membrane resting potential, or the rhythmic activity of neurons, increased HCN1 concentration in the pinceau can also improve the inhibitory effect on PCs and strongly regulate the outflow of information from the cerebellum, all of which is mediated by PCs. In human patients, disruptions of either HCN1 or Kvβ2 function in other brain regions were associated with epilepsy [48, 49].

In addition to life style effects, C57BL/6 mice showed innate vulnerability to kainate, reflected in extensive beading in the penumbra of the lesion, thicker axons and worse post-exposure beam walking performance than FVB/N mice. Lower levels of cation channels in the microenvironment of PCs attributed the better preservation of motor skills in FVB/N mice to this inherently higher PCs-adjacent support. Intriguingly, others demonstrated that the effects of peripheral KA injection were consistently more severe in FVB/N than in C57BL/6 mice, as evident by increased cell death in the hippocampus and extended epileptic behaviour [28, 50, 51]. Similarly, KA microinjection to the amygdala resulted in a more extensive cell death and epileptic seizures in FVB/N compared to C57BL/6 mice [52]. The relative resistance of the otherwise vulnerable FVB/N mice in our study may reflect different neuro-anatomical contexts (cerebellum *versus* hippocampus and amygdala), in which different sets and types of glutamate receptors and neurons exert different neurological impacts under intense glutamatergic stimulation. It may be interesting to compare the hippocampal Kir6.1 basal levels between FVB/N and C57BL/6 mice, because inheritably lower levels of Kir6.1 in the hippocampus can partially account for the increased vulnerability

of this brain structure in C57BL/6 mice to KA effects. Intriguingly, the excitotoxic hippocampal cell death in C57BL/6 mice was demonstrated as a multi-factorial trait determined by a complex interaction between a set of genes [50] and a recent study from the same group maps the responsible gene(s) to chromosome 15 [53]. We can assume that this gene(s) encodes a protein which is specifically involved in the hippocampal response to KA or otherwise that the cerebellum contains additional factors that counteract the non-specific effects of this gene's products.

The exercise-inducible reduction in serum AChE activity implies higher levels of ACh and possible suppression of cytokines production in leukocytes that might infiltrate into the brain. Alternatively, higher levels of circulation-originated ACh may penetrate the blood–brain barrier and interact with cerebellar microglia and α7nAChR-expressing BG, resulting in local reduction in cytokine production. That routine exercise attenuated kainate-induced expression of IL-6, MCP-1 and KC might hence be an additional mechanism by which exercise improves the short-term outcome after glutamate damage. However, certain pro-inflammatory cytokines have neurotrophic effects [54], suggesting that the long-term consequences of this attenuation is yet to be discovered.

Figure 6A and B summarizes the potential points of intervention which underlie the innate and exercise-mediated cerebellar resistance to glutamatergic excitotoxicity. Our results highlight similar molecular mechanisms as underlying the neuroprotective effects of genetic background and physical activity (exercise), and emphasize Kir6.1 as a potential target for new therapies and for tracing mutations in its encoding gene, KCNJ8. Further research is needed to determine the transcriptional and post-transcriptional events through which exercise mediates the increased expression of HCN1, KVβ2 and Kir6.1, clarify the physiological pathways through which enhanced expression of these channels improves resistance to glutamate toxicity and delineate the molecular mechanisms underlying the cholinergic-mediated and exercise-inducible regulation of brain cytokines and the inter-relations between them.

Acknowledgements

Conflict of interest

The authors confirm that there are no conflicts of interest.

Supporting information

Additional Supporting Information may be found in the online version of this article:

Fig. S1 Similar cation channels mediate protection by exercise and inheritance from cerebellar exitotoxicity.

Please note: Wiley-Blackwell is not responsible for the content or functionality of any supporting materials supplied by the authors. Any queries (other than missing material) should be directed to the corresponding author for the article.

References

1. **Karadottir R, Cavelier P, Bergersen LH**, *et al.* NMDA receptors are expressed in oligodendrocytes and activated in ischaemia. *Nature*. 2005; 438: 1162–6.

2. **Hurtado O, De Cristobal J, Sanchez V**, *et al.* Inhibition of glutamate release by delaying ATP fall accounts for neuroprotective effects of antioxidants in experimental stroke. *FASEB J*. 2003; 17: 2082–4.

3. **Slemmer JE, De Zeeuw CI, Weber JT.** Don't get too excited: mechanisms of glutamate-mediated Purkinje cell death. *RRRrog Brain Res*. 2005; 148: 367–90.

4. **Dirnagl U, Iadecola C, Moskowitz MA.** Pathobiology of ischaemic stroke: an integrated view. *Trends Neurosci*. 1999; 22: 391–7.

5. **Carro E, Trejo JL, Busiguina S**, *et al.* Circulating insulin-like growth factor I mediates the protective effects of physical exercise against brain insults of different etiology and anatomy. *J Neurosci*. 2001; 21: 5678–84.

6. **Galimanis A, Mono ML, Arnold M**, *et al.* Lifestyle and stroke risk: a review. *Curr Opin Neurol*. 2009; 22: 60–8.

7. **van Praag H.** Exercise and the brain: something to chew on. *Trends Neurosci*. 2009; 32: 283–90.

8. **Jordan BD.** Genetic influences on outcome following traumatic brain injury. *Neurochem Res*. 2007; 32: 905–15.

9. **Ben Assayag E, Shenhar-Tsarfaty S, Ofek K**, *et al.* Serum cholinesterase activities distinguish between stroke patients and controls and predict 12-month mortality. *Mol Med*. 16: 278–86.

10. **Neeper SA, Gomez-Pinilla F, Choi J**, *et al.* Exercise and brain neurotrophins. *Nature*. 1995; 373: 109.

11. **Ding C, He Q, Li PA.** Diabetes increases expression of ICAM after a brief period of cerebral ischemia. *J Neuroimmunol*. 2005; 161: 61–7.

12. **Petrilli V, Papin S, Dostert C**, *et al.* Activation of the NALP3 inflammasome is triggered by low intracellular potassium concentration. *Cell Death Differ*. 2007; 14: 1583–9.

13. **Wang Q, Yu S, Simonyi A**, *et al.* Kainic acid-mediated excitotoxicity as a model for neurodegeneration. *Mol Neurobiol*. 2005; 31: 3–16.

14. **Reiss JI, Dishman RK, Boyd HE***, et al.* Chronic activity wheel running reduces the severity of kainic acid-induced seizures in the rat: possible role of galanin. *Brain Res.* 2009; 1266: 54–63.

15. **Gobbo OL, O'Mara SM.** Exercise, but not environmental enrichment, improves learning after kainic acid-induced hippocampal neurodegeneration in association with an increase in brain-derived neurotrophic factor. *Behav Brain Res.* 2005; 159: 21–6.

16. **Ramsden M, Berchtold NC, Patrick Kesslak J***, et al.* Exercise increases the vulnerability of rat hippocampal neurons to kainate lesion. *Brain Res.* 2003; 971: 239–44.

17. **Seo TB, Kim BK, Ko IG***, et al.* Effect of treadmill exercise on Purkinje cell loss and astrocytic reaction in the cerebellum after traumatic brain injury. *Neurosci Lett.* 2010; 481: 178–82.

18. **Drab M, Haller H, Bychkov R***, et al.* From totipotent embryonic stem cells to spontaneously contracting smooth muscle cells: a retinoic acid and db-cAMP *in vitro* differentiation model. *Faseb J.* 1997; 11: 905–15.

19. **Brorson JR, Manzolillo PA, Gibbons SJ***, et al.* AMPA receptor desensitization predicts the selective vulnerability of cerebellar Purkinje cells to excitotoxicity. *J Neurosci.* 1995; 15: 4515–24.

20. **Sarna JR, Hawkes R.** Patterned Purkinje cell death in the cerebellum. *Prog Neurobiol.* 2003; 70: 473–507.

21. **Hamann M, Rossi DJ, Mohr C***, et al.* The electrical response of cerebellar Purkinje neurons to simulated ischaemia. *Brain.* 2005; 128: 2408–20.

22. **Matute C, Alberdi E, Domercq M***, et al.* Excitotoxic damage to white matter. *J Anat.* 2007; 210: 693–702.

23. **Bobik M, Ellisman MH, Rudy B***, et al.* Potassium channel subunit Kv3.2 and the water channel aquaporin-4 are selectively localized to cerebellar pinceau. *Brain Res.* 2004; 1026: 168–78.

24. **Schweighofer N, Doya K, Kuroda S.** Cerebellar aminergic neuromodulation: towards a functional understanding. *Brain Res Brain Res Rev.* 2004; 44: 103–16.

25. **Smith PD, Crocker SJ, Jackson-Lewis V***, et al.* Cyclin-dependent kinase 5 is a mediator of dopaminergic neuron loss in a mouse model of Parkinson's disease. *Proc Natl Acad Sci USA.* 2003; 100: 13650–5.

26. **Lee ST, Chu K, Jung KH***, et al.* Cholinergic anti-inflammatory pathway in intracerebral hemorrhage. *Brain Res.* 2010; 1309: 164–71.

27. **Goldstein LB.** Rapid reliable measurement of lesion parameters for studies of motor recovery after sensorimotor cortex injury in the rat. *J Neurosci Methods.* 1993; 48: 35–42.

28. **Yang J, Houk B, Shah J***, et al.* Genetic background regulates semaphorin gene expression and epileptogenesis in mouse brain after kainic acid status epilepticus. *Neuroscience.* 2005; 131: 853–69.

29. **Takeuchi H, Mizuno T, Zhang G***, et al.* Neuritic beading induced by activated microglia is an early feature of neuronal dysfunction toward neuronal death by inhibition of mitochondrial respiration and axonal transport. *J Biol Chem.* 2005; 280: 10444–54.

30. **Fan LW, Mitchell HJ, Rhodes PG***, et al.* Alpha-phenyl-*n*-tert-butyl-nitrone attenuates lipopolysaccharide-induced neuronal injury in the neonatal rat brain. *Neuroscience.* 2008; 151: 737–44.

31. **Soundarapandian MM, Zhong X, Peng L***, et al.* Role of K(ATP) channels in protection against neuronal excitatory insults. *J Neurochem.* 2007; 103: 1721–9.

32. **Hu LF, Wang S, Shi XR***, et al.* ATP-sensitive potassium channel opener iptakalim protected against the cytotoxicity of MPP+ on SH-SY5Y cells by decreasing extracellular glutamate level. *J Neurochem.* 2005; 94: 1570–9.

33. **Jansen LA, Uhlmann EJ, Crino PB***, et al.* Epileptogenesis and reduced inward rectifier potassium current in tuberous sclerosis complex-1-deficient astrocytes. *Epilepsia.* 2005; 46: 1871–80.

34. **De Filippi G, Baldwinson T, Sher E.** Nicotinic receptor modulation of neurotransmitter release in the cerebellum. *Prog Brain Res.* 2005; 148: 307–20.

35. **Gruol DL, Nelson TE.** Purkinje neuron physiology is altered by the inflammatory factor interleukin-6. *Cerebellum.* 2005; 4: 198–205.

36. **van Gassen KL, Netzeband JG, de Graan PN***, et al.* The chemokine CCL2 modulates Ca^{2+} dynamics and electrophysiological properties of cultured cerebellar Purkinje neurons. *Eur J Neurosci.* 2005; 21: 2949–57.

37. **Lax P, Limatola C, Fucile S***, et al.* Chemokine receptor CXCR2 regulates the functional properties of AMPA-type glutamate receptor GluR1 in HEK cells. *J Neuroimmunol.* 2002; 129: 66–73.

38. **Soreq H, Seidman S.** Acetylcholinesterase – new roles for an old actor. *Nat Rev Neurosci.* 2001; 2: 294–302.

39. **Wang Q, Tang XN, Yenari MA.** The inflammatory response in stroke. *J Neuroimmunol.* 2007; 184: 53–68.

40. **Rizzi M, Perego C, Aliprandi M***, et al.* Glia activation and cytokine increase in rat hippocampus by kainic acid-induced status epilepticus during postnatal development. *Neurobiol Dis.* 2003; 14: 494–503.

41. **Thomzig A, Laube G, Pruss H***, et al.* Pore-forming subunits of K-ATP channels, Kir6.1 and Kir6.2, display prominent differences in regional and cellular distribution in the rat brain. *J Comp Neurol.* 2005; 484: 313–30.

42. **Terry RD, Masliah E, Salmon DP***, et al.* Physical basis of cognitive alterations in Alzheimer's disease: synapse loss is the major correlate of cognitive impairment. *Ann Neurol.* 1991; 30: 572–80.

43. **Simard JM, Yurovsky V, Tsymbalyuk N***, et al.* Protective effect of delayed treatment with low-dose glibenclamide in three models of ischemic stroke. *Stroke.* 2009; 40: 604–9.

44. **Zhu HL, Luo WQ, Wang H.** Iptakalim protects against hypoxic brain injury through multiple pathways associated with ATP-sensitive potassium channels. *Neuroscience.* 2008; 157: 884–94.

45. **Sun XL, Zeng XN, Zhou F***, et al.* KATP channel openers facilitate glutamate uptake by GluTs in rat primary cultured astrocytes. *Neuropsychopharmacology.* 2008; 33: 1336–42.

46. **Nakahira K, Shi G, Rhodes KJ***, et al.* Selective interaction of voltage-gated K+ channel beta-subunits with alpha-subunits. *J Biol Chem.* 1996; 271: 7084–9.

47. **Maccaferri G, McBain CJ.** The hyperpolarization-activated current (Ih) and its contribution to pacemaker activity in rat CA1 hippocampal stratum oriens-alveus interneurones. *J Physiol.* 1996; 497(Pt 1): 119–30.

48. **Heilstedt HA, Burgess DL, Anderson AE***, et al.* Loss of the potassium channel beta-subunit gene, KCNAB2, is associated with epilepsy in patients with 1p36 deletion syndrome. *Epilepsia.* 2001; 42: 1103–11.

49. **Wierschke S, Lehmann TN, Dehnicke C***, et al.* Hyperpolarization-activated cation currents in human epileptogenic neocortex. *Epilepsia.* 2010; 51: 404–14.

50. **Schauwecker PE, Williams RW, Santos JB.** Genetic control of sensitivity to hippocampal cell death induced by kainic acid: a quantitative trait loci analysis. *J Comp Neurol.* 2004; 477: 96–107.

51. **Shikhanov NP, Ivanov NM, Khovryakov AV, et al.** Studies of damage to hippocampal neurons in inbred mouse lines in models of epilepsy using kainic acid and pilocarpine. *Neurosci Behav Physiol.* 2005; 35: 623–8.

52. **Kasugai M, Akaike K, Imamura S, et al.** Differences in two mice strains on kainic acid-induced amygdalar seizures. *Biochem Biophys Res Commun.* 2007; 357: 1078–83.

53. **Schauwecker PE.** Congenic strains provide evidence that a mapped locus on chromosome 15 influences excitotoxic cell death. *Genes Brain Behav.* 2011; 10: 100–10.

54. **Di Filippo M, Sarchielli P, Picconi B, et al.** Neuroinflammation and synaptic plasticity: theoretical basis for a novel, immune-centred, therapeutic approach to neurological disorders. *Trends Pharmacol Sci.* 2008; 29: 402–12.